Thermodynamic Properties and Swelling Behavior of Glycolipid Monolayers at Interfaces

Matthias F. Schneider, Gerald Mathe, and Motomu Tanaka*

Lehrstuhl für Biophysik E22, Technische Universität München, James-Franck-Strasse, D-85748 Garching, Germany

Christian Gege and Richard R. Schmidt

Fachbereich Chemie, Universität Konstanz, Fach M-725, D-78457 Konstanz, Germany

Received: August 2, 2000; In Final Form: January 22, 2001

Synthetic glycolipids with lactose headgroups ($N = 1$, 2, and 3) were synthesized, and their thermodynamic properties were systematically studied by Langmuir isotherms using a film balance. The molar transition entropy and the molar latent heat were calculated by applying the Clausius−Clapeyron equation. It has been demonstrated that the phase behavior of the glycolipid monolayers is comparable to that of ordinary phospholipids, despite the lower degree of cooperativity between the larger headgroups. The glycolipid monolayer was transferred onto a solid surface by Langmuir−Blodgett deposition, and the swelling behavior was investigated by ellipsometry. The surface grafting density was precisely controlled, and the water disjoining pressure inside the lactose layer was quantitatively measured. The measured swelling curves were analyzed in terms of the theoretical descriptions for the grafted polymer "brushes". For the lipids with lactose units of $N = 2$ and 3, the disjoining pressure−thickness relation could fit very well to these theoretical approaches, even though the statistical limit $N \gg 1$ is hardly fulfilled. The results suggest entropic effects of the headgroups on the interaction between the neighboring molecules. On the other hand, the theoretical description of the swelling behavior of the lipids with one lactose unit failed due to the "rodlike" structure of lactose. The unique properties of these glycolipids at interfaces, such as (i) the phase behavior comparable to that of ordinary phospholipids and (ii) the "polymer-like" swelling behavior, play very important roles in biological systems. Mimicking the complex interactions between oligosaccharide headgroups in the plasma membranes, the synthetic glycolipids designed in this study are quite realistic models for the glycocalix.

1. Introduction

Glycolipids, whose polar headgroups are attached to oligosaccharides, play fundamental and essential roles in cell−cell and cell−matrix interaction by (i) specific recognition by counterpart lectins, (ii) modulation of adhesion receptors, and (iii) glycolipid-glycolipid interaction.[1−7] For example, blood group- and tumor-associated antigens such as sialyl-Lewis-X and sialyl-Lewis-A interact specifically with selectins.[8,9] Although such phenomena have been widely studied, little is known regarding the interaction mechanism on a molecular level. Indeed, most of the experiments were concerned with the measurement of rather macroscopic quantities such as cell rolling assays to determine the rolling velocity and shear force resistance.[10−13]

It should be noted that such oligosaccharides only not serve as specific recognition sites but also provide a soft "cushion" between tissue-forming cells because of their unique swelling behavior.[14,15] To study the complex interplay of weak generic forces and strong specific forces, several artificial models have been proposed. Among various glycocalix models, phospholipids with poly(ethylene glycol) chains (PEG lipids) have been widely applied in numerous fields.[16] For example, vesicles doped with PEG lipids showed a remarkable increase in the blood circulation times compared with ordinary vesicles, corresponding to the steric repulsion by the PEG headgroups.[17−20] A similar approach has been chosen to stabilize the colloidal dispersions using the soft, hydrated chains.[21] Moreover, it has been reported that the PEG brushes grafted onto solid supports could passivate the surface against the nonspecific adsorption of the proteins.[22−25] There have been many reports on the effects of the ethylene glycol chain on their morphologies and interfacial properties;[26−33] however, quantitative studies of the thermodynamic and elastic properties of glycolipids themselves in the well-defined artificial model systems are still missing.

In the present study, lipids covalently attached to lactose oligomers (the number of lactose units, $N = 1$, 2, and 3) were synthesized, and their thermodynamic properties and swelling behavior were studied. Since each lactose unit takes a linear conformation, they are expected to be rather simple glycocalix models. The design of such well-defined biocompatible interfaces includes a variety of scientific applications toward the generation of cell and tissue surface models (e.g., basal laminas of blood vessels) to investigate the basic principles of cell adhesion and cell growth control.[34] Indeed, the glycolipid with a lactose spacer between sialyl-Lewis-X headgroup and a ceramide moiety exhibited similar efficiency in cell-rolling experiments.[13,35] In the first part of this study, Langmuir pressure−area isotherms were measured at several temperatures in order to estimate thermodynamic and structural parameters of the monolayers at the air/water interface. In the second part, glycolipid monolayers were transferred onto the hydrophilic

* Corresponding author. Tel: ++49-89-28912539. Fax: ++49-89-28912469. E-mail: mtanaka@ph.tum.de.

10.1021/jp0028103 CCC: $20.00
Published on Web 05/10/2001

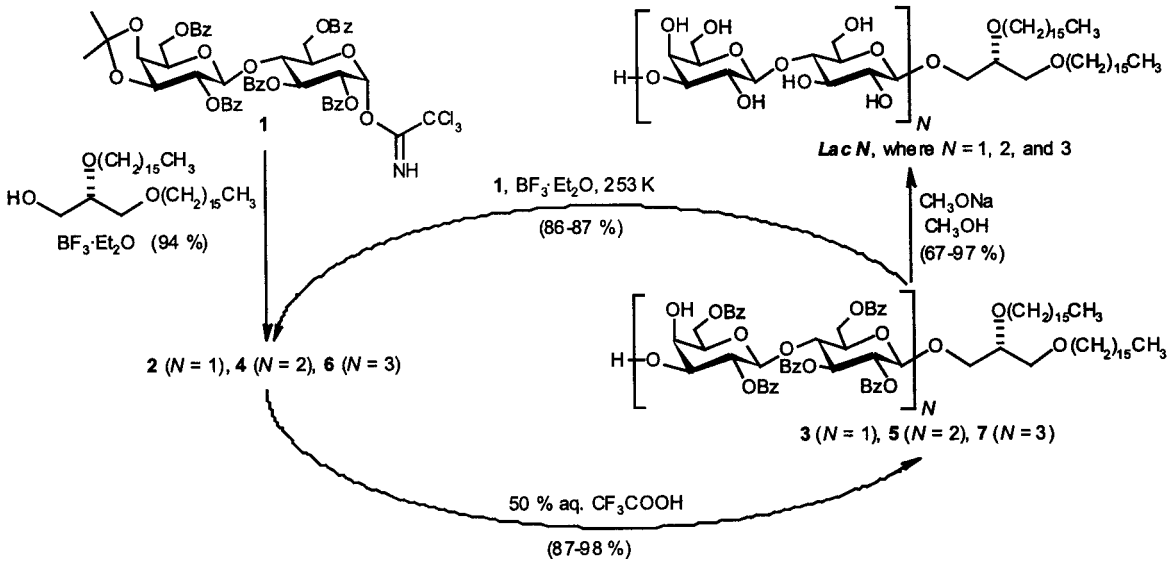

Figure 1. Synthesis of the investigated derivatives Lac *N* ($N = 1$, 2, and 3) via repetitive glycosylation.

silicon wafers. Equilibrium thickness of the saccharide layer was measured as a function of disjoining pressure by using ellipsometry. Relative humidity (i.e., partial water vapor pressure) in the measuring chamber was precisely controlled between 20% and 98%. The obtained results were discussed in terms of the scaling theory of de Gennes and Alexander[36−39] and a self-consistent field (SCF) approach of Milner.[40,41]

2. Materials and Methods

2.1. Synthesis of the Glycolipids. *2.1.1. General.* Solvents were purified according to the standard procedures. Flash chromatography was performed on J. T. Baker silica gel 60 (40−63 μm) or J. T. Baker RP-18 silica gel (40 μm) at a pressure of approximately 0.4 bar. Thin-layer chromatography was performed on Merck silica gel plastic plates $60F_{254}$ (TLC), glass plates $60F_{254}$ (HPTLC), or glass plates RP-18 $60F_{254S}$ (RP-18 TLC); compounds were visualized by UV light and charring with 15% aqueous H_2SO_4. Optical rotations were measured on a Perkin-Elmer polarimeter 241 in a 1 dm cell at 293 K. NMR measurement were recorded on a Bruker AC250 Cryospec or Bruker DRX spectrometer (using the deuterated solvent as internal standard, unless otherwise stated). The carbohydrate monomers were assigned in alphabetical order, beginning from the aglycon, based in part on carbon-proton shift-correlation heteronuclear multiple quantum coherence (HMQC); only the anomeric signals are shown. The water content of the glycolipids was calculated according elemental analysis.

2.1.2. Synthesis. In the following section, the investigated glycolipids were named Lac *N*, corresponding to the number of lactose units, $N = 1$, 2, and 3. The synthetic route to these glycolipids is shown in Figure 1: glycosidation of known lactose trichloroacetimidate **1**[42] with 1,2-di-*O*-hexadecyl-*sn*-glycerol[35,43] as lipid anchor was performed in the presence of $BF_3{\cdot}Et_2O$ as catalyst to afford the lactose intermediate **2** in 94% yield. The β-configuration of the newly formed glycosidic bond was confirmed in the ^{1}H NMR spectrum ($J_{1,2} = 7.9$ Hz). Acid-catalyzed cleavage of the isopropylidene group furnished **3**, which served as an acceptor for the next glycosylation. Removal of the *O*-benzoyl protective groups with sodium methoxide in CH_2Cl_2/CH_3OH afforded Lac 1 in almost quantitative yield after purification on reversed phase (RP-18) silica gel.

Elongation of **3** with donor **1** in the presence of $BF_3{\cdot}Et_2O$ as catalyst at 253 K afforded exclusively the expected β(1-3)-connected di-lactose intermediate **4** ($J_{1,2} = 7.9$ Hz for 1c−H; shift of the 4b−H signal from 3.85 to 5.29 ppm after acetylation). Again, de-*O*-isopropylidenation furnished the following acceptor **5**, and de-*O*-benzoylation furnished the desired Lac 2 derivative under the conditions described above. Repetitive coupling of **5** with donor **1** yielded the elongated protected glycolipid **6**, which was de-*O*-isopropylidenated in the same manner. Because of the low solubility of Lac 3, the de-*O*-benzoylation and purification were performed in dimethyl sulfoxide (DMSO) mixtures.

(1,2-Di-O-hexadecyl-sn-3-glyceryl)-O-(2,6-di-O-benzoyl-3,4-di-O-isopropylidene-β-D-galactopyranosyl)-(1→4)-2,3,6-tri-O-benzoyl-β-D-glucopyranoside (2). A solution of (2,6-di-*O*-benzoyl-3,4-di-*O*-isopropylidene-β-D-galactopyranosyl)-(1 → 4)-2,3,6-tri-*O*-benzoyl-β-D-glucopyranosyl trichloroacetimidate **1**[42] (3.81 g, 3.64 mmol) and 1,2-di-*O*-hexadecyl-*sn*-glycerol[35,43] (1.97 g, 3.64 mmol) in dry CH_2Cl_2 (25 mL) was treated at room temperature with $BF_3{\cdot}Et_2O$ (138 μL, 1.09 mmol). After stirring for 15 min, the mixture was neutralized with NEt_3 and concentrated in vacuo. Flash chromatography on silica with a mixture of toluene/ethyl acetate (12/1) as eluent afforded **2** (4.88 g, 94%) as a colorless solid. TLC (10/1 toluene/ethyl acetate) $R_f = 0.39$. mp 377 K. $[\alpha]_D = 28.4$ ($c = 1.0$ in $CHCl_3$).^{1}H NMR (250 MHz, $CDCl_3$): δ 4.72 (d, $J_{1,2} = 7.9$ Hz, 1H; 1a−H).

(1,2-Di-O-hexadecyl-sn-3-glyceryl)-O-(2,6-di-O-benzoyl-β-D-galactopyranosyl)-(1→4)-2,3,6-tri-O-benzoyl-β-D-glucopyranoside (3). Compound **2** (410 mg, 287 μmol) was dissolved in CH_2Cl_2 (5 mL), and 50% aqueous CF_3COOH (5 mL) was added. After stirring vigorously for 6 h, the mixture was diluted with CH_2Cl_2 (50 mL). The organic phase was washed with a saturated aqueous $NaHCO_3$ solution, dried (Na_2SO_4), and concentrated. The residue was purified by flash chromatography (eluent: 4/1 toluene/acetone) to give **3** (392 mg, 98%) as colorless foam. TLC (4/1 toluene/acetone) $R_f = 0.32$. $[\alpha]_D = 27.2$ ($c = 1.0$ in $CHCl_3$).

(1,2-Di-O-hexadecyl-sn-3-glyceryl)-O-(β-D-galactopyranosyl)-(1→4-β-D-glucopyranoside (Lac 1). A solution of sodium methoxide (1 M) in CH_3OH (1.7 mL) was added to a solution of **3** (600 mg, 433 μmol) in dry CH_3OH and dry CH_2Cl_2 (40 mL each). After stirring overnight, the solution was neutralized with Amberlite IR120 (H^+), filtered, and absorbed on RP-18 silica. Flash chromatography on RP-18 silica with a mixture of 0/4/1 → 0/1/0 → 65/25/4 $CHCl_3/CH_3OH/H_2O$ as eluent afforded

Lac 1 (419 mg, 97%) as a colorless powder after lyophilization from H_2O/dioxane (3/1). HPTLC (80/20/2 $CHCl_3/CH_3OH/H_2O$) $R_f = 0.58$. $[\alpha]_D = -12.3$ ($c = 1.0$ in 65/25/4 $CHCl_3/CH_3OH/H_2O$). ^1H NMR (600 MHz, TMS, 65/25/4 $CDCl_3/CD_3OD/D_2O$): δ 4.29 (d, $J_{1,2} = 7.8$ Hz, 1H; 1a−H), 4.33 (d, $J_{1,2} = 7.0$ Hz, 1H; 1b−H). $C_{47}H_{92}O_{13}\cdot H_2O$ (883.3).

(1,2-Di-O-hexadecyl-sn-3-glyceryl)-O-(2,6-di-O-benzoyl-3,4-di-O-isopropylidene-β-D-galactopyranosyl)-(1→4)-(2,3,6-tri-O-benzoyl-β-D-glucopyranosyl)-(1→3)-(2,6-di-O-benzoyl-β-D-galactopyranosyl)-(1→4)-2,3,6-tri-O-benzoyl-β-D-glucopyranoside (4). A solution of **1** (160 mg, 153 μmol)[42] and **3** (193 mg, 139 μmol) in dry CH_2Cl_2 (2 mL) was treated at 253 K with $BF_3\cdot Et_2O$ (5.3 μL, 42 μmol). After stirring for 15 min, the mixture was neutralized with NEt_3 and concentrated in vacuo. Flash chromatography (eluent: 10/1 toluene/acetone) afforded **4** (275 mg, 87%) as a colorless foam. TLC (9/1 toluene/acetone) $R_f = 0.36$. $[\alpha]_D = 42.1$ ($c = 1.0$ in $CHCl_3$). ^1H NMR (600 MHz, $CDCl_3$): δ 4.45 (d, $J_{1,2} = 7.9$ Hz, 1H; 1d−H), 4.57 (d, $J_{1,2} = 7.6$ Hz, 1H; 1b−H), 4.62 (d, $J_{1,2} = 7.9$ Hz, 1H; 1c−H), 4.68 (d, $J_{1,2} = 7.9$ Hz, 1H; 1a−H).

(1,2-Di-O-hexadecyl-sn-3-glyceryl)-O-(2,6-di-O-benzoyl-β-D-galactopyranosyl)-(1→4)-(2,3,6-tri-O-benzoy-β-D-glucopyranosyl)-(1→3)-(2,6-di-O-benzoyl-β-D-galactopyranosyl)-(1→4)-2,3,6-tri-O-benzoyl-β-D-glucopyranoside (5). Compound **4** (2.85 g, 1.25 mmol) was treated as described for **3** to give after flash chromatography (eluent: 5/1 toluene/acetone) derivative **5** (2.63 g, 94%) as colorless foam. TLC (4/1 toluene/acetone) $R_f = 0.30$. $[\alpha]_D = 45.2$ ($c = 1.0$ in $CHCl_3$).

(1,2-Di-O-hexadecyl-sn-3-glyceryl)-O-(β-D-galactopyranosyl)-(1→4)-(β-D-glucopyranosyl)-(1→3)-(β-D-galactopyranosyl)-(1→4)-β-D-glucopyranoside (Lac 2). A solution of sodium methoxide (1 M) in CH_3OH (1.8 mL) was added to a solution of **5** (199 mg, 88.5 μmol) in dry CH_3OH (40 mL). After stirring overnight, the solution (with precipitate) was evaporated and dissolved in $CHCl_3/CH_3OH/H_2O$ (65/25/4). After neutralization with Amberlite IR120 (H^+), the solvent was filtered and absorbed on RP-18 silica. Flash chromatography on RP-18 silica with a mixture of 0/3/1 → 0/1/0 → 65/25/4 $CHCl_3/CH_3OH/H_2O$ as eluent afforded Lac 2 (85.5 mg, 80%) as a colorless powder after lyophilization from H_2O/dioxane (3/1). HPTLC (70/30/4 $CHCl_3/CH_3OH/H_2O$) $R_f = 0.49$. $[\alpha]_D = 0.6$ ($c = 1.0$ in 65/25/4 65/25/4$CHCl_3/CH_3OH/H_2O$). ^1H NMR (600 MHz, TMS, 65/25/4 $CDCl_3/CD_3OD/D_2O$): δ 4.30 (d, $J_{1,2} = 8.2$ Hz, 1H; 1a−H), 4.37 (t, 1H; 1d−H), 4.44 (d, $J_{1,2} = 7.7$ Hz, 1H; 1b−H), 4.57 (d, $J_{1,2} = 7.7$ Hz, 1H; 1c−H). $C_{59}H_{112}O_{23}\cdot H_2O$ (1207.5).

(1,2-Di-O-hexadecyl-sn-3-glyceryl)-O-(2,6-di-O-benzoyl-3,4-di-O-isopropylidene-β-D-galactopyranosyl)-(1→4)-(2,3,6-tri-O-benzoyl-β-D-glucopyranosyl)-(1→3)-(2,6-di-O-benzoyl-β-D-galactopyranosyl)-(1→4)-(2,3,6-tri-O-benzoyl-β-D-glucopyranosyl)-(1→3)-(2,6-di-O-benzoyl-β-D-galactopyranosyl)-(1→4)-2,3,6-tri-O-benzoyl-β-D-glucopyranoside (6). A solution of **1** (540 mg, 513 μmol)[42] and **5** (958 mg, 429 μmol) in dry CH_2Cl_2 (8 mL) was treated at 253 K with $BF_3\cdot Et_2O$ (16 μL, 129 μmol), and then the ice bad was removed. After stirring for 30 min, the mixture was neutralized with NEt_3 and concentrated in vacuo. Flash chromatography (eluent: petroleum ether/ethyl acetate $^2/_1$ → $^3/_2$) afforded **6** (1.15 g, 86%) as a colorless foam. TLC (petroleum ether/ethyl acetate 2/1) $R_f = 0.20$. $[\alpha]_D = 56.8$ ($c = 1.0$ in $CHCl_3$). ^1H NMR (600 MHz, $CDCl_3$): δ 4.40 (d, $J_{1,2} = 8.0$ Hz, 1H; 1b−H), 4.43 (d, $J_{1,2} = 8.0$ Hz, 1H; 1d−H), 4.56−4.58 [m, 2H. HMQC: 4.56 (1c−H), 4.58 (1f−H)], 4.60 (d, $J_{1,2} = 7.9$ Hz, 1H; 1a−H), 4.67 (d, $J_{1,2} = 7.8$ Hz, 1H; 1e−H).

(1,2-Di-O-hexadecyl-sn-3-glyceryl)-O-(2,6-di-O-benzoyl-β-D-galactopyranosyl)-(1→4)-(2,3,6-tri-O-benzoyl-β-D-glucopyranosyl)-(1→3)-(2,6-di-O-benzoyl-β-D-galactopyranosyl)-(1→4)-(2,3,6-tri-O-benzoyl-β-D-glucopyranosyl)-(1→3)-(2,6-di-O-benzoyl-β-D-galactopyranosyl)-(1→4)-2,3,6-tri-O-benzoyl-β-D-glucopyranoside (7). Compound **6** (1.11 g, 356 μmol) was treated as described for **3** to give after flash chromatography (eluent: 3/1 toluene/acetone) derivative **7** (958 mg, 87%) as colorless foam. TLC (3/1 toluene/acetone) $R_f = 0.34$. $[\alpha]_D = 48.9$ ($c = 1.0$ in $CHCl_3$).

(1,2-Di-O-hexadecyl-sn-3-glyceryl)-O-(β-D-galactopyranosyl)-(1→4)-(β-D-glucopyranosyl)-(1→3)-(β-D-galactopyranosyl)-(1→4)-(β-D-glucopyranosyl)-(1→3)-(β-D-galactopyranosyl)-(1→4)-β-D-glucopyranoside (Lac 3). A solution of sodium methoxide (1 M) in CH_3OH (3.3 mL) was added to a solution of **7** (402 mg, 131 μmol) in dry CH_3OH and dry DMSO (10 mL each). The solution was stirred for 3 days, diluted with some water, and absorbed on RP-18 silica. Flash chromatography on RP-18 silica with a mixture of 0/1 → 2/1 → 1/1 → 1/2 DMSO/H2O as eluent afforded Lac 3 (136 mg, 67%) as a colorless powder after lyophilization from H_2O. RP-18 TLC (1/2 DMSO/CH_3OH) $R_f = 0.14$.

2.2. Sample Preparation. Thermally oxidized silicon wafers were given as a gift from Wacker Chemtronic (Burghausen, Germany). Freshly distilled ultrapure water (Millipore, Molsheim, France) was used as a subphase throughout this study. All other chemicals were purchased from Fluka (Neu-Ulm, Germany) and used without further purification. The spreading solutions were prepared by dissolving each glycolipid into the mixture of chloroform/methanol (70/30 by volume) at a concentration of 1×10^{-3} M.

2.3. Film Balance Experiments. Langmuir pressure−area isotherms were measured with a film balance designed in our laboratory (trough area: 982.5 cm^2). After the lipids were spread onto the subphase, the surface pressure was monitored with a Wilhelmy plate in the course of compression at a rate of 1.3 cm^2/min. The whole trough was temperature-controlled with a commercially available heating/cooling system. Typical errors in temperature control were in the range of ±0.5 K.

2.4. Static Swelling Measurements. Equilibrium thickness of the glycolipid monolayer deposited onto hydrophilic Si/SiO_2 substrates by the Langmuir−Blodgett method was measured as a function of relative humidity using a conventional point ellipsometer (Plasmos GmbH Prozesstechnik, München, Germany). The ellipsometer was attached to a film balance equipped with a closed chamber, which enables precise control of the relative humidity of the atmosphere between 4% and 98% (Figure 2). Throughout the experiment, a constant flow (5 L/min) of the adjusted humid air was applied. During the spreading and compression of the monolayer, a vertically mounted Si/SiO_2 substrate remained dipped in the subphase. After the surface pressure reached to a well-defined pressure value of $p = 25$ mN/m, the substrate was pulled out from the subphase at a rate of ~0.1 mm/s. The total thickness of the deposited monolayer, which consists of the lactose layer and the layer of the alkyl chains, was measured at a constant wavelength ($\lambda = 632.8$ nm) and a fixed angle of incidence (70°). Thickness of the lactose layer was calculated by assuming the alkyl layer thickness of 1.8 nm and the refractive index of $n = 1.5$.[31−33] By measuring the two ellipsometric angles, Ψ and Δ, we can derive the ratio between the complex reflection coefficients, R_p/R_s,

$$R_p/R_s = \tan \Psi \exp(-i\Delta) \qquad (1)$$

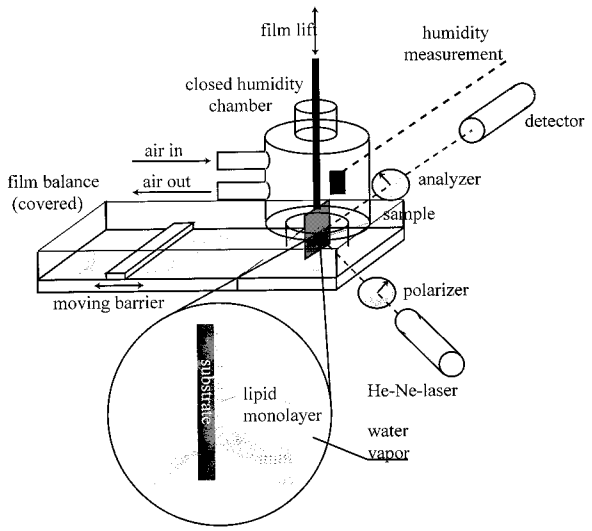

Figure 2. Schematic drawing of the ellipsometer coupled to a covered film balance and a humidity chamber. The top of the chamber was sealed with an o-ring, and bottom was connected to the covered film balance. The glycolipid monolayer could be transferred onto the substrate by the Langmuir−Blodgett method. By mixing dry air and water-saturated air, the relative humidity inside the chamber was controlled between 4% and 98%. The flow rate was 5 L/min, and the chamber volume was about 3 L.

R_p and R_s are given as the ratio between the incident and evanescent electric fields; $R_p = E_{p,evan}/E_{p,incid}$, and $R_s = E_{s,evan}/E_{s,incid}$. The initial thickness of the monolayer (i.e., thickness under low humidity conditions) was determined between 4% and 20% of relative humidity. The thickness change in this regime was in the range of the resolution limit of the ellipsometer used (1−2 Å). Between two subsequent equilibrium thickness measurements, the film was allowed to equilibrate for about 10 min. Furthermore, the thickness was measured at decreasing humidity as well as at increasing humidity to ensure the equilibrium between the deposited monolayer and the humid air. A refractive index of $n = 1.56$ for the bulk polysaccharide was assumed[32,44−46] to evaluate the initial thickness of the lactose layer by analyzing R_p/R_s in terms of the Fresnel equations.[47]

For the thickness evaluation of the swollen lactose film containing increasing amounts of water, the refractive index was calculated by applying the Garnet equation,[48,49] which relates the refractive index of a homogeneous solution, n_F, to the volume fraction of the solute, Φ

$$n_F = n_M \sqrt{1 + \frac{3\Phi}{\left(\frac{n_0^2 + 2n_M^2}{n_0^2 - n_M^2}\right) - \Phi}} \qquad (2)$$

n_0 and n_M are the refractive indices of the pure solute and the pure solvent, respectively. The volume fraction Φ is simply related to the layer thickness d by $\Phi = d_0/d$, where d_0 is the initial film thickness. The equilibrium film thickness at certain humidity can be calculated self-consistently, starting from the refractive index of the initial layer and successively applying the Garnet formula.

The dominating forces between these two interfaces separated by a thin lactose layer can be described in the context of the disjoining pressure model.[50] This external pressure, p, can be defined as the negative derivative of Gibbs free energy G, with respect to the film thickness d, $p = -\partial G/\partial d$. G is the free energy of the film, which is a function of the thickness d and the water volume fraction within the film.[51,52] The disjoining pressure can be expressed by use of van't Hoffs law

$$p = -\left(\frac{RT}{V_m}\right)\ln(X) \qquad (3)$$

where V_m is the molar volume of water, T is the temperature. R stands for the gas constant, and X is the relative humidity inside the chamber. To analyze the force−distance relationship within this interlayer, we plotted the determined layer thickness as a function of the relative humidity (i.e., disjoining pressure), yielding the disjoining pressure-thickness curve.

3. Theoretical Concepts

The measured swelling curves were analyzed by applying two different physical concepts: (i) the scaling theory by Alexander and de Gennes[36−39] and (ii) the mean field approach by Milner.[40,41] Although our experimental systems do not fulfill a symmetrically planar situation with the polymers confined between two parallel plates, all the equations discussed in the following chapter were applicable to the experimental data by multiplying all theoretical expressions by the order of unity.

3.1. Scaling Theory. A general expression for the free energy F of grafted polymers on the surface is given by de Gennes, Alexander, and Daoud[36−39] by

$$F \approx kTN\left(\frac{a}{D}\right)^{5/3} - \delta\left(\frac{Na}{D}\right) + \delta\left(\frac{Na^3}{\sigma D}\right)^{5/4} + kT\left(\frac{D}{a}\right)^2\left(\frac{\xi}{a}\right)^{-1/3}N^{-1} + kT\ln\sigma \qquad (4)$$

N is the number of monomer segments with length a, and D is the thickness of the polymer layer. δ represents the surface adsorption energy per monomer in units of kT, while σ and ξ the mean area per polymer and the blob diameter, respectively.[38] The first term describes the energy necessary to confine a polymer molecule behaving as an ideal chain inside a blob. The second term stands for the adsorption energy of a chain on the surface, while the third term for the repulsion between overlapped polymer chains. The fourth term describes the so-called "brush" regime. The last term represents the translational entropy of the polymers, which can be neglected by assuming that the alkyl chains are immobilized on the surface.

In case the distance between the grafting points d_p is less than the Flory radius, $d_p < R_F$, the polymer chain takes a "brush" conformation with the blob diameter of ξ. The equilibrium thickness D^{st}_{brush} can be described as $D^{st}_{brush} \approx aNd_p^{-2/3}$. The interaction potential of the polymer V^{st}_{brush} is given by

$$V_{brush} \approx \frac{kT}{d_p^3}D^{st}_{brush}\left[\frac{4}{5}\left(\frac{D^{st}_{brush}}{D}\right)^{5/4} + \frac{4}{7}\left(\frac{D}{D^{st}_{brush}}\right)^{7/4}\right] \qquad (5)$$

yielding the resulting pressure of

$$P^{st}_{brush} \approx \frac{kT}{d_p^3}\left[\left(\frac{D^{st}_{brush}}{D}\right)^{9/4} - \left(\frac{D}{D^{st}_{brush}}\right)^{3/4}\right] \qquad (6)$$

3.2. Self-Consistent-Field Approach. The self-consistent-field (SCF) approach of Milner et al.[40,41] is based on the terminally fixed linear chains exhibiting a high grafting density.

In contrast to the scaling approach, the quality of the solvent is not so crucial in this treatment. When the film is compressed from the equilibrium thickness $D_{\text{brush}}^{\text{scf}}$, the interaction energy per unit area can be described as

$$V_{\text{brush}}^{\text{scf}} \approx -\left(\frac{\pi^2}{12}\right)N(\sigma w)^{2/3}\left[\frac{D_{\text{brush}}^{\text{scf}}}{2D} + \frac{1}{2}\left(\frac{D}{D_{\text{brush}}^{\text{scf}}}\right)^2 - \frac{1}{10}\left(\frac{D}{D_{\text{brush}}^{\text{scf}}}\right)^5\right] \quad (7)$$

and the resulting interfacial pressure is given by

$$P_{\text{brush}}^{\text{scf}} \approx \left(\frac{\pi^2}{12}\right)N(\sigma w)^{2/3}\frac{1}{D_{\text{brush}}^{\text{scf}}}\left[-\frac{1}{2}\left(\frac{D_{\text{brush}}^{\text{scf}}}{D}\right)^2 + \frac{D}{D_{\text{brush}}^{\text{scf}}} - \frac{1}{2}\left(\frac{D}{D_{\text{brush}}^{\text{scf}}}\right)^4\right] \quad (8)$$

$\sigma = d_p^{-2}$ is the grafting density, and w stands for the "excluded volume".

4. Results and Discussion

4.1. Langmuir Isotherms. For each glycolipid (the number of lactose units, $N = 1, 2, 3$), the pressure−area isotherms were measured at several different temperature conditions between 283 and 308 K. To eliminate hysteresis effects, we monitored the isotherms during the expansion as well as during the compression.

The Langmuir isotherms of the Lac 1 lipid are shown in Figure 3a. At $T \leq 298$ K, the isotherms exhibited no liquid expanded phase and were dominated by the condensation of the dihexadecyl chains from a gas phase to a liquid condensed phase. Such behavior can be explained by the stiffness of the short, fully hydrated, and stretched "rodlike" lactose moieties. At $T = 303$ K, an onset of a plateaulike regime was observed, corresponding to a first-order phase transition from the liquid expanded to the liquid condensed state. Further rise in temperature leads to an increase in the transition pressure and a decrease in the coexistence region. Such a systematic tendency coincides with the approach to a critical point, which is well-known from the previous studies on ordinary phospholipid monolayers.[53,54]

As presented in Figure 3b,c, qualitatively similar isotherms were observed for the monolayers of Lac 2 and Lac 3. In accordance with the increase in the lactose units, a systematic increase in the transition pressure, p_K, at a given temperature was observed (Figure 4a). The obtained results suggested that the steric interactions between neighboring lipid molecules were dominated by the strong repulsion between the headgroups. However, the qualitative shape of the coexistence region was still dominated by the lateral packing density of the alkyl chains and not by the "polymer-like" effects of the headgroups. Indeed, a similar tendency was observed in the previous study for the monolayers of PEG lipids with shorter chains.[33]

It should be also noticed that the slope of the isotherms in the coexistence region was increased with the increase in the size of the lactose headgroups. Such a slope in the Langmuir isotherms can be generally explained by the stabilization of domains due to (i) small amounts of impurities (≥0.2 mol %),[55,56] (ii) "intermediate" states of the alkyl chains,[57] or (iii) the strong interaction between the headgroups.[58] The first two approaches are based on nonequilibrium effects, which do not follow the Gibbs phase rule; however, the third interpretation explains this slope by the continuous compression of the headgroups. From a thermodynamic point of view, any slope can be described by a decrease in cooperativity of the transition, while a classical first-order transition assumes infinite cooperativity. Therefore, it is plausible that the larger headgroups result in a less effective interaction between the alkyl chains.

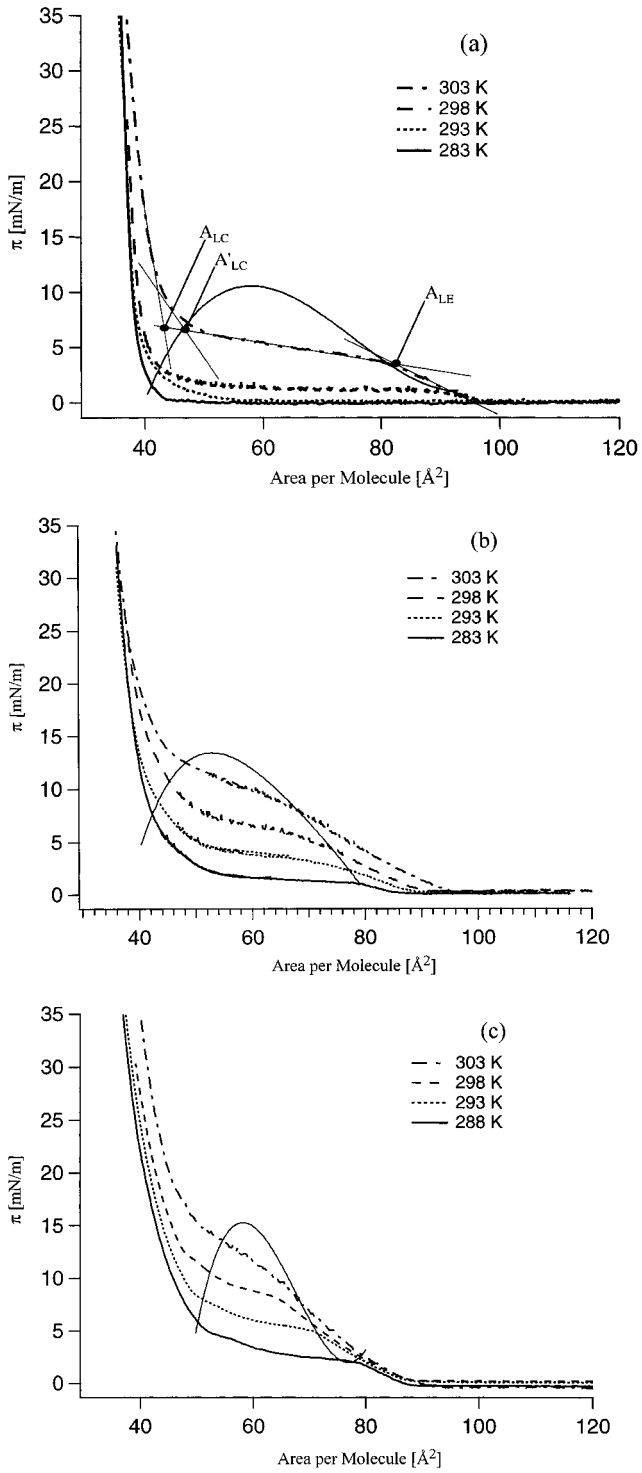

Figure 3. Langmuir isotherms of the monolayers of (a) Lac 1 at $T =$ 283, 293, 298, and 303 K, (b) Lac 2 at $T = 288$, 293, 298, and 303 K, and (c) Lac 3 at $T = 288$, 293, 298, and 303 K. The fluid−gas coexistence line was fitted by polynomial of 4th order (broken line). At high temperature and pressure conditions, the coexistence line can be approximated as parabola, whose vertex coincides with the critical point. The points of intersection of the linear extrapolated lines in panel a were taken to define A_{LE} and A_{LC}. To estimate the deviation in A, we took several points.

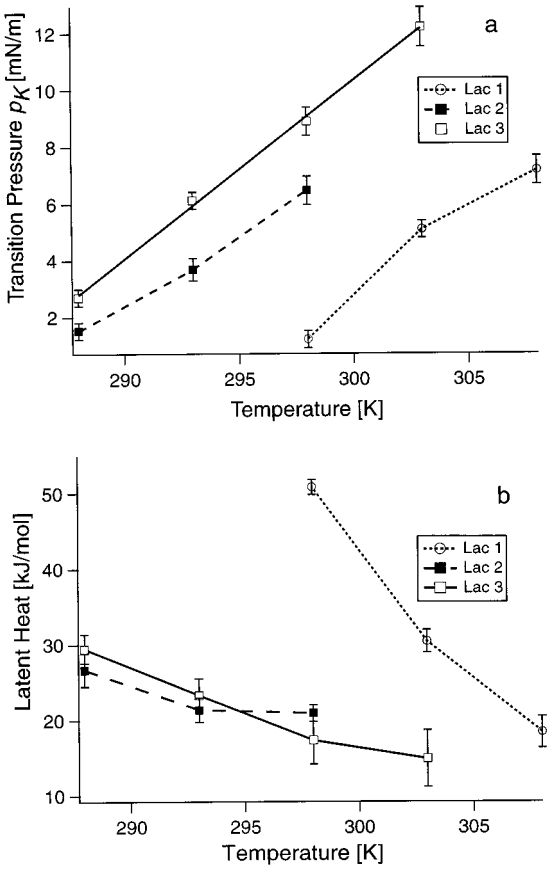

Figure 4. (a) Transition pressure p_K and (b) molar latent heat of the phase transition q plotted as a function of temperature T for Lac 1 (open circle), Lac 2 (closed square), and Lac 3 (open square).

By applying the Clausius−Clapeyron equation

$$\frac{dp_K}{dT} = \frac{\Delta s}{(A_{LE} - A_{LC})} = \frac{\Delta q}{T(A_{LE} - A_{LC})} \tag{9}$$

we can estimate thermodynamic quantities such as the molar latent heat, q, or the molar transition entropy, $s = q/T$, from the variation of the transition pressure with the absolute temperature, dp_K/dT. It should be noted that the values $A_{LE} - A_{LC}$ and Δq can differ up to 50%, depending on how the onset (A_{LE}) and the end point (A_{LC}) of the transition were defined. As shown in Figure 3a, we defined the onset and the end point according to the manner previously reported.[59,60] The increase in p_K as well as the decrease in $A_{LE} - A_{LC}$ with temperature observed in this study had been also reported for phospholipid monolayers, and they can be understood in terms of a two-dimensional van der Waals gas model. The phase coexistence region can be fitted by polynomial of 4th order (Figure 3 a−c). At high surface pressure and high temperatures, the phase coexistence line can be approximated well as a parabola, whose vertex coincides with the critical point. This justifies, at least as a rough estimation, the application of a two-dimensional van der Waals equation in the vicinity of this critical point. Expanding of the van der Waals equation near the critical point derives

$$\frac{A - A_C}{A_C} = 2\left(\frac{T_C - T}{T_C}\right)^{1/2} \tag{10}$$

where A_C is the area at the maximum of the parabola.[61] From

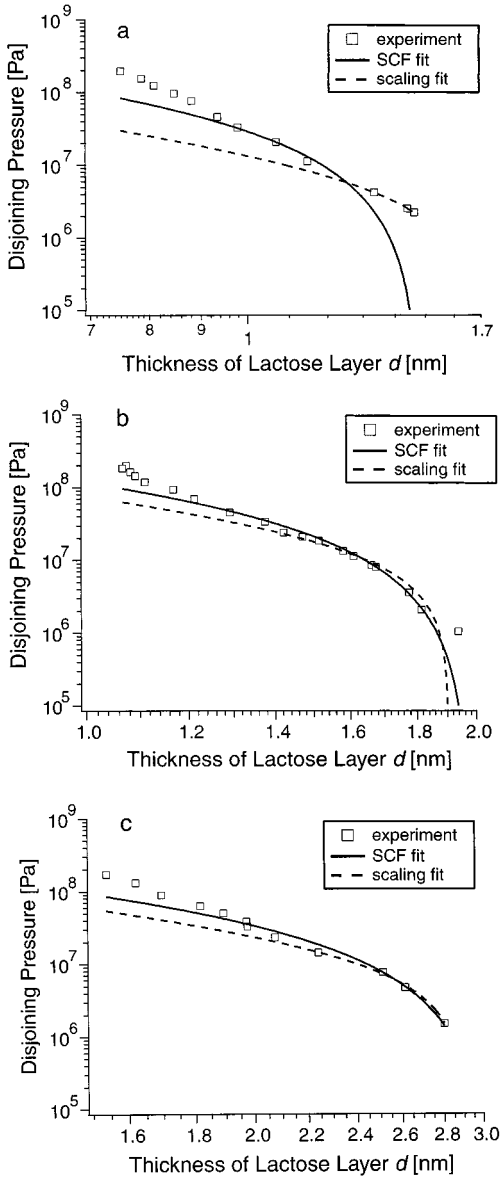

Figure 5. Absolute disjoining pressure vs thickness of the lactose layers for (a), Lac 1, (b) Lac 2, and (c) Lac 3. The measured values (open circles) were compared with the theoretical predictions based on the self-consistent-field approach (solid lines) and the scaling theory (broken lines). The swelling behavior of Lac 2 and Lac 3 could be well explained by both of the "brush" models.

the linear assumption between p_K and T (Figure 4a), the critical pressure can be derived from the critical temperature, T_C, calculated according to eq 10. This leads to a critical pressure $p_C = 9-16$ mN/m and a critical temperature of $T_C = 313-316$ K, respectively. The extracted values were in good agreement with the critical pressure derived from the parabola fit, which also supports the validity of our theoretical model. Moreover, they are also comparable to those of phospholipids with dihexadecyl chains.[54] Figure 4b shows the temperature dependence of the latent heat Δq. When the lactose moiety was longer, the corresponding latent heat was less than that of the shorter one, which can be attributed to the lower degree of cooperativity due to the larger headgroups.

4.2. Swelling Behavior of Glycolipid Monolayers. The glycolipid monolayers were transferred onto the substrate at $T = 293$ K and at a lateral pressure of $p = 25$ mN/m. The areas per molecule were 37 Å^2 (Lac 1), 37 Å^2 (Lac 2), and 40 Å^2 (Lac 3), respectively. In this regime, the glycolipids take the

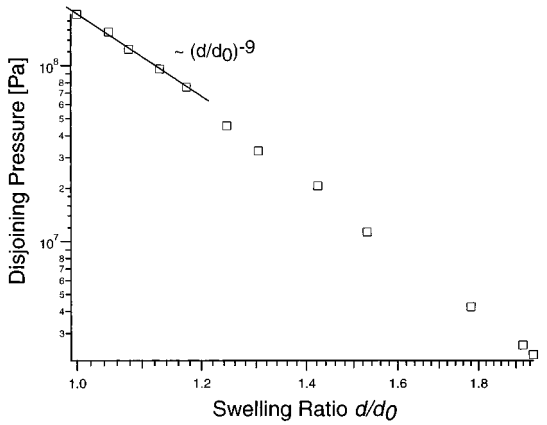

Figure 6. Absolute disjoining pressure as a function of relative swelling ratio of Lac 1, d/d_0, normalized to the thickness of "dry" layer. At high disjoining pressures from 2×10^8 to 7×10^7 Pa, a power law $p \propto (d/d_0)^n$ was fitted to the disjoining pressure curves, yielding an exponent of $n \approx -9$.

liquid condensed phase, where the alkyl chains orient nearly perpendicular to the surface. The relative humidity was varied between 30% and 98%, corresponding to a change of the disjoining pressure between 1.69×10^9 and 2.83×10^6 Pa.

In Figure 5a−c, the disjoining pressure is plotted versus the absolute thickness of the swollen lactose layer. In each plot, both the experimental data (open squares) as well as two theoretical fits are presented based on the scaling approach and the SCF model. To expose possible power law dependence between the disjoining pressure against the thickness, we presented all results as log−log plot. The swelling behavior of Lac 1 could hardly be interpreted as "brushes" neither by the scaling approach nor by the SCF theory, even though the swelling ratio of ∼2.0 in the low-pressure regime (∼10^7 Pa) is still in a plausible range from the corresponding ratios of dextran (∼2.0) and hyaluronic acid (∼2.7).[46] This observation suggests that the very short headgroups behave like "rigid-rod" but not like "polymer chains", similar to what had been observed for the PEG lipid monolayers with shorter chains.[33] This is also in a good agreement with the Langmuir isotherms of Lac 1, showing the qualitatively similar characteristics to phospholipid monolayers. At high disjoining pressures from 2×10^8 to 7×10^7 Pa, a power law $p \propto (d/d_0)^n$ was fitted to the disjoining pressure curves, yielding an exponent of $n \approx -9$ (Figure 6). In this high disjoining pressure regime, typical intermolecular distances, r, are comparable to Bohr radius (∼0.5 Å), and the swelling should be mainly dominated by short-range repulsive interactions caused by the overlapping of molecular orbitals. The hard core repulsion of the Lennard−Jones potential scales as r^{-12}. This exponent corresponds to a scaling law of $p \propto (d/d_0)^{-9}$ [50] that agrees with the power law obtained from our experiments. Similar power law dependencies in the high disjoining pressure regime could be also observed for Lac 2 and Lac 3.

In Figure 5b,c, the swelling behaviors of Lac 2 and Lac 3 were compared with theoretical predictions for "polymer brushes" based on the scaling approach and the SCF theory. Indeed, both of the "brush" models fit obviously better to the measured disjoining pressure curves than the "mushroom" models, which is quite evident from the conditions of preparations (i.e., high transfer pressure, relatively short headgroups). Also, it should be noted that the thickness of the lactose layers (≤3 nm) is still far away from the basic statistical condition, $N \gg 1$. These results also showed a good agreement with results for PEG lipids with longer chains.[33]

The difference between the swelling behavior of Lac 1 from those of Lac 2 and Lac 3 might be explained by the influence of the alkyl chains on the phase transition of the glycolipid monolayers. Actually, the Langmuir isotherms of Lac 1 were dominated by the condensation of the alkyl chains at $T \leq 298$ K (Figure 3a). In accordance with the increase in the lactose units, the headgroups gained conformational entropy. The steric interaction between the neighboring lipids is strongly influenced by the repulsion between headgroups. Thus, the swelling curves could be well explained by the "brush like" behavior of the lactose groups.

5. Conclusions

Interfacial properties of the synthetic glycolipids with lactose headgroups (Lac N; $N = 1$, 2, and 3) were systematically studied by applying two experimental techniques. Thermodynamic and structural properties were obtained from film balance experiments. The Langmuir isotherms clearly show an increase in the transition pressure and in the slope of the transition regime, according to the increasing number of lactose units. This reflects the increase in the repulsion between headgroups, which impedes upon the compression of alkyl chains as well as an increase in the solubility, which in turn causes a decrease in cooperativity. From the phase coexistence regions in the isotherms, the molar transition entropy, s, and the molar latent heat, q, were estimated by applying the Clausius−Clapeyron equation. Furthermore, by applying a two-dimensional van der Waals gas model, the critical temperature and the critical pressure were estimated, $T_C = 313-316$ K and $p_C = 9-16$ mN/m, respectively. It is worth noting that the phase behavior of the glycolipid monolayers is comparable to that of ordinary phospholipids, despite the lower degree of cooperativity between the larger headgroups.

The swelling behaviors of these lipids were investigated by ellipsometry coupled to a film balance and a humidity chamber, which enables the precise control of the surface grafting density and the quantitative measurements of the water disjoining pressure inside the lactose layer. Theoretical interpretation was attempted by applying the scaling theory and the SCF approach for the grafted polymer "brushes". Both of the theoretical treatments failed to explain the disjoining pressure−thickness relation of the Lac 1 monolayer. This might be due to the "rodlike" structure of lactose. For Lac 2 and Lac 3, the swelling curves could be fitted very well by these theoretical approaches, suggesting entropic effects of the headgroups on the interaction between the neighboring molecules. The random conformations of the lactose groups resulted in the "polymer-like" swelling behavior, driven by the water uptake of the saccharide layer.

As described above, the unique properties of these glycolipids at the interface can be specified in terms of (i) the dominating effects of alkyl chains on the phase behavior, which is comparable to that of ordinary phospholipids, and (ii) the specific swelling behavior due to the hydration, which can be interpreted as that of "polymer brushes". The first characteristics is very important in biological systems to keep the cell membrane structure stable, while the second plays a key role to form a soft "cushion", preventing the nonspecific adhesion between cells and tissues. For the study of the complex interplay of various physical forces in the cell−cell recognition processes, the synthetic glycolipids designed here are quite unique and suitable glycocalix models. The quantitative study of the various generic forces at biocompatible interfaces includes a variety of scientific applications toward the generation of models of cell

and tissue surfaces to investigate the basic principles of the interactions between oligosaccharide headgroups in plasma membranes.

Acknowledgment. The authors express the deepest gratitude to Prof. Erich Sackmann for his constant support and helpful suggestions throughout this work. We are also grateful to Dr. Armin Geyer for his help in the structural assignments by NMR experiments. We appreciate Wacker Chemtronic (Burghausen, Germany) for providing thermally oxidized silicon wafers as a gift. This work was supported by the Deutsche Forschungsgemeinschaft (DFG Sa 246/27-2, Schm 213/36-2) and the Fonds der Chemischen Industrie. One of the authors (M. T.) is an Alexander von Humboldt Fellow.

References and Notes

(1) Curatolo, W. *Biochim. Biophys. Acta* **1987**, *906*, 137.
(2) Hakomori, S. *Pure Appl. Chem.* **1991**, *63*, 473.
(3) Hakomori, S.; Igarashi, Y. *J. Biochem.* **1995**, *118*, 1091.
(4) Springer, T. A. *Annu. Rev. Physiol.* **1995**, *57*, 827.
(5) Gabius, H. J.; Gabius, S. *Glycoscience*; Chapmann & Hall: Weinheim, 1997.
(6) Geyer, A.; Gege, C.; Schmidt, R. R. *Angew. Chem., Int. Ed. Engl.* **1999**, *38*, 1466.
(7) Geyer, A.; Gege, C.; Schmidt, R. R. *Angew. Chem., Int. Ed. Engl.* **2000**, *39*, 3246.
(8) Feizi, T. *Curr. Opin. Struct. Biol.* **1993**, *3*, 701.
(9) Varki, A. *Proc. Natl. Acad. Sci. U.S.A.* **1994**, *91*, 7390.
(10) Lawrence, M. B.; Springer, T. A. *Cell* **1991**, *65*, 859.
(11) Goetz, D. J.; Brandley, B. K.; Hammer, D. A. *Ann. Biomed. Eng.* **1996**, *24*, 87−98.
(12) Brunk, D. K.; Goetz, D. J.; Hammer, D. A. *Biophys. J.* **1996**, *71*, 2902−2907.
(13) Vogel, J.; Bendas, G.; Bakowsky, M.; Hummel, G.; Schmidt, R. R.; Kettmann, U.; Rothe, U. *Biochim. Biophys. Acta* **1998**, *1372*, 205.
(14) Andrade, S. *Surface and Interfacial Aspects of Biomedical Polymers*; Plenum Press: New York, 1985.
(15) Israelachvili, J. N.; Wennerström, H. *Nature* **1996**, *379*, 219.
(16) Harris, J. M. *Poly(ethyleneglycol*) *Chemistry*; Plenum Press: New York, 1992.
(17) Blume, G.; Cevc, G. *Biochim. Biophys. Acta* **1990**, *1029*, 91.
(18) Kilbanov, A. L.; Maruyama, K.; Torchilin, V. P.; Huang, L. *FEBS Lett.* **1990**, *268*, 235.
(19) Papahadjopoulos, D.; Allen, T. M.; Gabizon, A.; Mayhew, E.; Matthay, K.; Huang, S. K.; Lee, K.-D.; Woodle, M. C.; Lasic, D. D.; Redemann, C.; Martin, F. J. *Proc. Natl. Acad. Sci. U.S.A.* **1991**, *88*, 11460.
(20) Wu, N. Z.; Da, D.; Rudoll, T. L.; Needham, D.; Whorton, A. R.; Dewhirst, M. W. *Cancer Res.* **1993**, *53*, 3765.
(21) Napper, D. H. *Polymeric Stability of Colloidal Dispersions*; Academic Press: New York, 1983.
(22) Lee, J. H.; Kopecek, J.; Andrade, S. *J. Biomed. Mater. Res.* **1989**, *23*, 351.
(23) Bridgett, M. J.; Davies, M. C.; Dencer, S. P. *Biomaterials* **1992**, *13*, 411.
(24) Desai, N. P.; Hossainy, S. F. A.; Hubbell, J. A. *Biomaterials* **1992**, *13*, 417.
(25) Yang, Z.; Galloway, J. A.; Yu, H. *Langmuir* **1999**, *15*, 8405.
(26) Kuhl, T. L.; Leckband, D. E.; Lasic, D. D.; Israelachvili, J. N. *Biophys. J.* **1994**, *66*, 1479.
(27) Kenworthy, A. K.; Simon, S. A.; McIntosh, T. J. *Biophys. J.* **1995**, *68*, 1903.
(28) Kenworthy, A. K.; Hristova, K.; Needham, D.; McIntosh, T. J. *Biophys. J.* **1995**, *68*, 1921.
(29) Kuhl, T. L.; Majewski, J.; Wong, J. Y.; Steinberg, S.; Leckband, D. E.; Israelachvili, J. N.; Smith, G. S. *Biophys. J.* **1998**, *75*, 2352.
(30) Naumann, C. A.; Brooks, C. F.; Fuller, G. G.; Knoll, W.; Frank, C. W. *Langmuir* **1999**, *15*, 7752.
(31) Baekmark, T. R.; Elender, G.; Lasic, D. D.; Sackmann, E. *Langmuir* **1995**, *11*, 3975.
(32) Elender, G. Ph.D. Thesis, Technische Universität München, München, Germany, 1996.
(33) Mathe, G.; Gege, C.; Neumaier, K. R.; Schmidt, R. R.; Sackmann, E. *Langmuir* **2000**, *16*, 3835.
(34) Sackmann, E.; Tanaka, M. *Trends Biotechnol.* **2000**, *18*, 58.
(35) Gege, C.; Bendas, G.; Vogel, J.; Rothe, U.; Schmidt, R. R. *Chem. Eur. J.* **2000**, *6*, 111.
(36) De Gennes, P. G. *J. Phys.* **1976**, *37*, 1445.
(37) Alexander, S. *J. Phys. II France* **1977**, *38*, 983−987.
(38) De Gennes, P. G. *Macromolecules* **1980**, *13*, 1069−1075.
(39) Daoud, M.; De Gennes, P. G. *J. Phys. II* **1977**, *38*, 85−93.
(40) Milner, S. T.; Witten, T. A.; Cates, M. E. *Macromolecules* **1988**, *21*, 2610−2619.
(41) Milner, S. T.; Witten, T. A.; Cates, M. E. *Europhys. Lett.* **1988**, *5*, 413−418.
(42) Lay, L.; Windmüller, R.; Reinhardt, S.; Schmidt, R. R. *Carbohydr. Res.* **1997**, *303*, 39.
(43) Abdelmageed, O. H.; Duclos, R. I., Jr.; Griffin, R. G.; Siminovitch, D. J.; Ruocco, M. J.; Makriyannis, A. *Chem. Phys. Lipids* **1989**, *50*, 163.
(44) Elender, G.; Kühner, M.; Sackmann, E. *Biosens. Bioelectron.* **1996**, *11*, 565−577.
(45) In *Handbook of Chemistry and Physics*; Lide, D. R., Ed.; CRC Press Inc.: New York, 1997.
(46) Mathe, G.; Albersdörfer, A.; Neumaier, K. R.; Sackmann, E. *Langmuir* **1999**, *15*, 8726.
(47) Azzam, R. M. A.; Bashara, N. M. *Ellipsometry and Polarized Light*; North Holland: Amsterdam, 1977.
(48) Garnet, M. *Philos. Trans. R. Soc. London, Ser. A* **1904**, *203*, 385−420.
(49) Garnet, M. *Philos. Trans. R. Soc. London, Ser. A* **1906**, *205*, 237−288.
(50) Israelachvili, J. N. *Intermolecular and Surface Forces*, 2nd ed.; Academic Press: London, 1992.
(51) Rand, R. P. *Annu. Rev. Biophys. Bioeng.* **1981**, *10*, 277−314.
(52) Landau, L. D.; Lifschitz, E. M. *Lehrbuch der theoretischen Physik, Band V, Statistische Physik Teil1*, 7th Auflage ed.; Akademie-Verlag: Berlin, 1987.
(53) Albrecht, O.; Gruler, H.; Sackmann, E. *J. Phys.* **1978**, *39*, 301−313.
(54) Möhwald, H. In *Structure and Dynamics of Membranes*; Lipowsky, R., Sackmann, E. H., Ed.; Elsevier: Amsterdam, 1995.
(55) Pallas, N. R.; Pethica, B. A. *Langmuir* **1985**, *1*, 509.
(56) Miller, A.; Möhwald, H. *J. Chem. Phys.* **1987**, *86*, 4258.
(57) Mouritsen, O. G. *Biochim. Biophys. Acta* **1983**, *731*, 217.
(58) Scott, H. L., Jr. *Biochim. Biophys. Acta* **1975**, *406*, 329.
(59) Köberl, M.; Hinz, H.-J. R.; G. *Chem. Phys. Lipids* **1997**, *85*, 23−43.
(60) Johann, C.; Garidel, P.; Mennicke, L.; Blume, A. *Biophys. J.* **1996**, *72*, 3215−3228.
(61) Goldenfeld, N. *Lectures on Phase Transitions and the Renormalization Group*; Addiso-Wesley Publishing: Reading, MA, 1992.